Available online at www.sciencedirect.com
ScienceDirect
Catalysis Today 126 (2007) 103–111
CATALYSIS TODAY
www.elsevier.com/locate/cattod

Combining computational and in situ spectroscopies joint with molecular modeling for determination of reaction intermediates of *de*NO_x process—CuZSM-5 catalyst case study

Piotr Pietrzyk [a,*], Barbara Gil [a], Zbigniew Sojka [a,b,**]

[a] *Faculty of Chemistry, Jagiellonian University, ul. Ingardena 3, 30-060 Krakow, Poland*
[b] *Regional Laboratory of Physicochemical Analyses and Structural Research, Jagiellonian University, ul. Ingardena 3, 30-060 Krakow, Poland*

Available online 13 November 2006

Abstract

Interaction of NO with Cu^{I}ZSM-5 catalysts was spectroscopically investigated in static (IR and EPR) and flow (IR) regimes, complemented by DFT quantum chemical calculations. Particular attention was paid to the elucidation of the N–N bond formation mechanism, which (along with O–O bond making) is one of the key issues of a *de*NO_x reaction. The active sites ({Cu^{I}}ZSM-5, {CuO}ZSM-5), the intermediates ({$Cu^{I}NO$}ZSM-5}, {$Cu^{I}N_2O_2$}ZSM-5}), and the low-temperature spectators (up to 423 K) ({$Cu^{I}(NO)_2$}ZSM-5}) appearing during this process were identified. Their assignment and molecular structure was ascertained by joint use of computational spectroscopy and DFT modeling. A new method of discrimination between the conformers of surface dinitrosyls based on the calculations of the relative IR intensities of the symmetric and antisymmetric vibrations was proposed, and the mechanistic importance of copper dinitrosyl conformation was discussed. The inner-sphere versus outer-sphere mechanistic dichotomy of the N–N bond conception was rationalized in terms of the spin density repartition within the Cu–NO moiety of the mononitrosyl intermediate.

Keywords: NO dimer; Dinitrosyl; Hyponitrate; IR intensity; CuZSM-5; *de*NO_x mechanism; IR; EPR; DFT

1. Introduction

Despite of being thermodynamically favored, catalytic abatement of NO_x still remains a challenging problem from both fundamental and practical point of view [1–4]. A number of important mechanistic issues concerning the nature of the active sites and the key intermediates, as well as the molecular level description of the reaction elementary steps have not been definitely resolved yet. In this context wide scientific interest in the CuZSM-5 zeolite stems from its remarkable activity in direct NO decomposition, and the advantage of exhibiting a relatively simple structure. This makes CuZSM-5 a convenient model system for basic mechanistic studies and quantum chemical calculations [5–8]. DFT modeling of heterogeneous catalytic systems is, however, computationally quite demanding. Judicious selection of an appropriate cluster model and an adequate calculation scheme is of great importance for obtaining sensible results. In our method of exploring the mechanism of catalytic reactions we combine molecular modeling with computational spectroscopy. Spectroscopic parameters of postulated active sites, reaction intermediates and spectators are calculated and directly compared with available experimental data (EPR magnetic parameters, IR frequencies and intensities). Such approach provides a quantitative bridge between the spectroscopic fingerprints of the investigated species and their molecular structure and reactivity [9].

The backbone of a *de*NO_x process over CuZSM-5 zeolites can be epitomized in the form of two interconnected cycles associated with the formation of N_2 and O_2. The principal mechanistic steps include the formation of a N–N bond, where NO reactant is transformed into N_2O intermediary product, and simultaneously the primary {Cu^{I}}Z active sites are converted

* Corresponding author. Tel.: +48 12 663 22 24; fax: +48 12 634 05 15.
** Corresponding author at: Faculty of Chemistry, Jagiellonian University, ul. Ingardena 3, 30-060 Krakow, Poland. Tel.: +48 12 663 22 95; fax: +48 12 634 05 15.
E-mail addresses: pietrzyk@chemia.uj.edu.pl (P. Pietrzyk), sojka@chemia.uj.edu.pl (Z. Sojka).

0920-5861/$ – see front matter © 2006 Elsevier B.V. All rights reserved.
doi:10.1016/j.cattod.2006.09.033

into the secondary {CuO}Z sites, involved next in the dioxygen cycle [6]. The copper(I) mononitrosyl complexes are usually postulated to be the key intermediate species of this step [1,6,10], whereas the role of the dinitrosyls is not clearly established as yet. Decomposition of N_2O into the constituent elements can occur either via oxygen transfer to the copper-oxo centers, restoring the initial active sites, or to the remaining intact $\{Cu^I\}Z$ centers. This step is supposed to require a molecular transport of N_2O between various active sites [6]. Oxidation of gas-phase NO on copper-oxo centers leads to NO_2, which is the central intermediary product of the O–O bond formation cycle, involving copper nitrates as the key intermediates [3,6,14]. During the whole process the active sites alternate between the primary $\{Cu^I\}Z$ and the secondary {CuO}Z centers, which drives both N_2 and O_2 reaction cycles. While alternative scenarios involving dinuclear active sites also exist [11–13], we focus on the well defined model involving the {Cu}Z/{CuO}Z couple, and by assuming these entities to be active species we develop a consistent mechanistic description of NO decomposition process.

In the present work our interest was focused on the elucidation of molecular mechanism of the N–N bond formation step of the *de*NO_x reaction, catalyzed by mononuclear copper centers hosted in ZSM-5 zeolite. Such sites can be prepared in a well-defined state as described elsewhere [14]. The specific goal was to identify the key intermediates involved in the N–N bond making, discriminate them from deceive or spectator species, and provide a molecular rational of the observed structure–reactivity relationship. We combine DFT calculations joint with computational spectroscopy to support the interpretation of the in situ pulse static and flow-condition IR and EPR measurements and to guide the mechanistic modeling.

2. Experimental

CuZSM-5 samples were obtained from parent NH_4ZSM-5 zeolite (Zeolyst, Inc., with SiO_2/Al_2O_3 ratio equal to 30) by classic ion exchange from 0.1 M $Cu(NO_3)_2$ aqueous solution. pH of the mixture was adjusted to 4. One gram of the zeolite was contacted with 100 cm^3 of the parent solution and stirred at 323 K for 20 h. IR measurements in flow and static regimes were performed using a home-made quartz cell with ZnSe windows. The cell was placed in the Bruker Equinox 55 spectrometer, equipped with an MCT detector allowing for a spectral resolution of 2 cm^{-1}. Prior to the measurements, the samples (ca. 20 mg) prepared in the form of self-supporting wafers were activated in vacuum (0.13 Pa) at 823 K. Static, 10 μmol pulse adsorption experiments were carried out at 153, 303, and 423 K. The NO decomposition reaction was performed in the temperature range of 298–823 K in the flow of 1% NO/He gas mixture (Linde Gas Polska) with GHSV of 24,000 h^{-1}. Static X-band EPR spectra were recorded with Bruker ELEXYS 500 machine using a rectangular TE_{102} cavity with 100 kHz modulation. EPR parameters were determined by computer simulation with EPRsim32 program [15].

DFT calculations were carried out by means of DMol [16] software using BPW [17] exchange-correlation functional and DNP basis set. Various cluster models of increasing size used for the quantum chemical investigations were cut-off from ZSM-5 structure [18] and terminated with OH groups. We have epitomized the Cu^IZSM-5 sites with the following clusters: $Cu^I[Si_2AlO_2(OH)_8]^-$ (Cu^I–**I2**), $Cu^I[Si_4AlO_5(OH)_{10}]^-$ (Cu^I–**M5**), $Cu^I[Si_5AlO_6(OH)_{12}]^-$ (Cu^I–**Z6**), and $Cu^I[Si_6AlO_8(OH)_{12}]^-$ (Cu^I–**M7**). Their localization within the ZSM-5 framework and more detailed description can be found in our earlier papers [9,19]. Vibrational analysis was performed within the double-harmonic approximation. The Hessian matrices were evaluated by numerical differentiation of the analytic energy gradients. To be directly compared with experimental IR results, the calculated harmonic frequencies were corrected by a scaling factor (NO_{exptl}/NO_{DFT}) to account for the anharmonicity. For the stretching mode, this factor was derived from the frequency of the free NO molecule, since it fits the experimental data quite well [20]. The ratio of the experimental to the computed harmonic frequencies for the NO molecule was equal to 1876/1843 = 1.018. Calculations of the hyperfine coupling constants were performed with the Gaussian98 program [21] for the previously optimized cluster structures. We used BPW91 functional together with 6–311G(*d*) and LanL2DZ basis sets. The ***g*** tensors were obtained from the spin-unrestricted zero order regular approximation (ZORA) [22] implemented in the ADF software [23] within the VWN LSDA calculation scheme. In the paper we use a notation $\{Cu^n(NO)_n\}$ZSM-5 or its abbreviated form $\{Cu^n(NO)_m\}$Z, where *n* indicates the formal oxidation state of copper, while Z stands for the ZSM-5 host.

3. Results and discussion

3.1. Intrazeolitic coordination chemistry of NO-pulse IR experiments

The static IR spectra obtained upon adsorption of NO at 153 K on the thermally preactivated CuZSM-5 are shown in Fig. 1a. After introduction of a 10 μm pulse of NO a band located at 1814 cm^{-1} prevailed in the spectrum. It is characteristic of the well known paramagnetic mononitrosyl adduct $\{Cu^INO\}$ZSM-5 [24–26]. However, with the increasing number of NO doses, a new doublet signal with the components at 1825 and 1730 cm^{-1} developed, becoming rapidly dominant. The position of those peaks are characteristic of the geminal dinitrosyl $\{Cu^I(NO)_2\}$ZSM-5 complex [5,14]. Such surface species were previously recognized in various Cu-exchanged zeolites, and their formation is manifested by the presence of two collective vibrations of the nitrosyl ligands, giving rise to symmetric (1825 cm^{-1}) and antisymmetric (1730 cm^{-1}) stretchings [24–26]. The structure of the $\{Cu^I(NO)_2\}$ZSM-5 complex is discussed in detail in the next section. The two sets of bands appeared simultaneously, though after a second NO dose the intensity of the mononitrosyl band strongly decreased to eventually vanish at higher coverage. Subsequent evacuation of the sample at 220 K led to a gradual decrease in the intensity

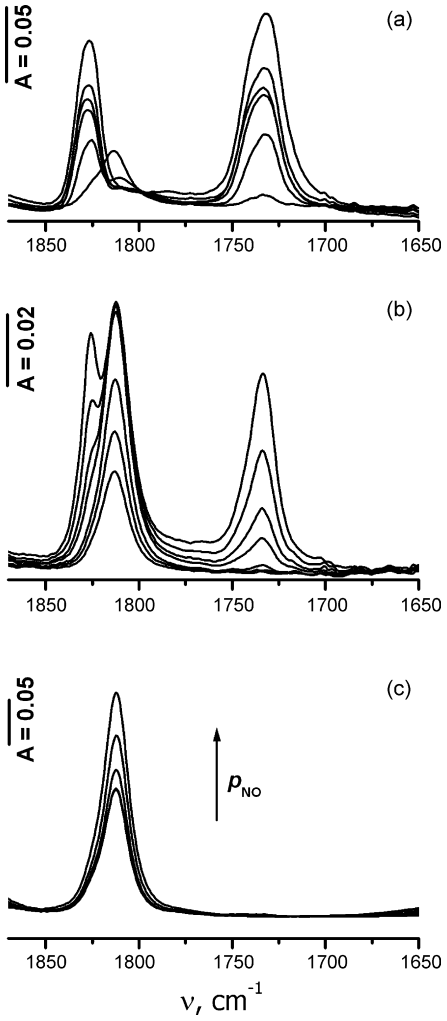

Fig. 1. IR spectra obtained after 10 μmol pulse adsorption of NO on CuZSM-5 recorded at: (a) 153 K, (b) 303 K, and (c) 423 K.

of the copper dinitrosyl bands, which was accompanied by a parallel recovery of the mononitrosyl peak, indicating a reversible transformation of both cage complexes. However, lack of a clear isosbestic point suggests that those reactions may occur in a parallel-consecutive manner (Scheme 1).

A similar pulse experiment carried out at 303 K (Fig. 1b) led initially to the development of the mononitrosyl band, but at higher coverage a doublet of the dinitrosyl complex grew up progressively. The mono- and dinitrosyl complexes remained in mutual equilibrium, that could be easily shifted by varying the number of NO doses, provided that $NO_{(g)}$ pressure was kept small. On the contrary, at 423 K, out of the two copper nitrosyls only the band due to the {Cu^{I}NO}ZSM-5 adduct ($\upsilon = 1814$ cm^{-1}) was present, regardless the number of NO pulses (Fig. 1c). This indicated that dinitrosyls were essentially unstable at such conditions. Indeed, a marked difference in the adsorption energies, −35.1 kcal/mol for {Cu^{I}}Z + NO → {Cu^{I}NO}Z and

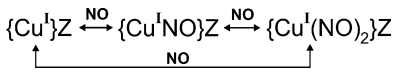

Scheme 1.

−18.2 kcal/mol for {Cu^{I}NO}Z + NO → {Cu^{I}(NO)$_2$}Z, obtained from our DFT calculations, can fully account for this observation. In addition, in the low frequency region, a weak pattern characteristic of copper nitrites and nitrates [27,28] emerged, gaining in the intensity with the increasing number of NO pulses.

Except of the bands discussed above, other complex but rather weak absorption with the components at 1910, 1904, and 1895 cm^{-1} (not shown in the figure) was observed and attributed to cage complexes of NO with Cu^{II} ions [28]. Its intensity increased with the increasing temperature and pressure until 303 K, but at these conditions it was not related to the concomitant evolution of the NO complexes with the monovalent copper. However, at 423 K the growth of the {Cu^{II}NO}ZSM-5 band with the increasing NO pressure was accompanied by partial decrease of that due to the {Cu^{I}NO}ZSM-5 complex. This indicated that at low temperatures the {Cu^{II}NO}ZSM-5 species were probably produced out of the residual Cu^{II} ions, i.e., those not reduced in the course of thermal activation, whereas at higher temperatures part of the monovalent copper is oxidized by NO as discussed elsewhere in more detail [5,24]. The above findings remain in a full agreement with the earlier literature data [5,6,29]. Thus, from the collation of the IR results, we may infer that upon temperature increase the dinitrosyls are merely converted (reversibly) into the mononitrosyls, but without formation of any other product relevant for the postulated catalytic cycle, provided that no gas-phase NO is present in substantial amounts.

Since the copper dinitrosyl complexes are essentially unstable at the temperatures above 223 K, they involvement in the NO decomposition over CuZSM-5 as the intermediates of the N–N bond formation process is uncertain, despite some earlier claims [24,29]. This problem was approached by means of in situ IR measurements of a working catalyst discussed in the next sections.

3.2. NO decomposition followed by in situ IR studies

A different picture emerged from the comparison of the in situ IR measurements in the static and flow conditions. The IR spectra recorded in the temperature range of 423–823 K during the catalytic reaction of NO with the CuZSM-5 sample under the isothermal flow conditions are collected in Fig. 2. The spectra are dominated by the broad and intense absorption bands centered at 1470, 1630, and 2224 cm^{-1}, assigned to NO_2-related species such as surface nitrates NO_3^- [30,31], nitrites NO_2^- [28,29] and to N_2O intermediary product, respectively. Their intensity gradually dropped with the increasing temperature. In comparison to the static measurements recorded at the same temperature of 423 K (Fig. 2, inset), the band due to the {Cu^{I}NO}ZSM-5 adducts was quite weak, and no traces of the dinitrosyls could be distinguished. Such behavior indicates that once gas-phase NO is present, the {Cu^{I}NO}ZSM-5 species are readily consumed (their concentration dropped distinctly below the thermal stability level at the same temperature), undergoing a transformation into the intermediate products of the successive *de*NO_x reaction steps, such as N_2O and $NO_{2(3)}$ species. Thus, it may be concluded that

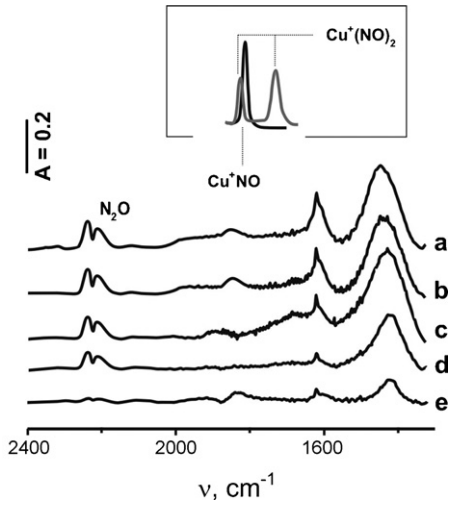

Fig. 2. In situ flow condition IR spectra recorded at: (a) 423 K, (b) 523 K, (c) 573 K, (d) 673 K, and (e) 823 K, during the reaction of 1% NO in He with CuZSM-5 at GHSV = 24,000 h^{-1}. In the inset static spectra at 303 K (dinitrosyl) and 423 K (mononitrosyl) are shown.

the transformation of nitric oxide into N_2O does not involve the dinitrosyl complexes but apparently requires the presence of the gaseous NO reactant.

To clarify the role of the mono- and dinitrosyl complexes as the intermediates in the N–N bond making step, it is necessary to develop a more in-depth insight into the structure–reactivity relationship for both adducts, and to understand the possible ways of attaching the second NO molecule to the {Cu^I–NO}ZSM-5 complex.

3.3. Insight into molecular structure of copper nitrosyl complexes through computational spectroscopy

The mononitrosyls are assigned on the basis of their spectroscopic fingerprints: the monoclinic EPR spectrum with $g_{xx} = 1.999$, $g_{yy} = 2.003$, $g_{zz} = 1.889$, $A_{xx} = 16.5$ mT, $A_{yy} = 15.5$ mT, $A_{zz} = 20.5$ mT, and the NO stretching vibration $\nu_{NO} = 1814$ cm^{-1}. The electronic and magnetic structure of this adduct was thoroughly investigated by means of computational spectroscopy in our previous papers, and the molecular origin of the hyperfine coupling [19] and the ***g*** tensor anisotropy [9] is well understood at present. The considerable agreement between theory and experiment of both magnetic and vibration parameters (Table 1) allowed for ascertaining the molecular structure of the copper mononitrosyl intermediate consistently. The ensuing MO rationale of the Cu–NO binding showed that the unpaired electron remains on the NO ligand. Because the charge of the copper center is quite well distributed over the zeolite framework, the Cu cation becomes softer and its 4s level is brought closer to the 3d manifold allowing for partial 4s – $3d_{z^2}$ hybridization. This opens the closed 3d shell of the tripodal Cu^I, permitting mixing of the copper 3d orbitals with the $2\pi^*$ orbitals of the NO ligand. The resultant new reactive spin distribution within the {Cu^INO} moiety with the spin density accumulated on the nitrogen atom is crucial in accounting for the outer-sphere mechanism of the N–N bond formation.

For making the N–N bond one obviously needs two NO molecules brought into an intimate contact. Conceivably, there are two possible mechanistic pathways for attachment of the next NO molecule to the mononitrosyl intermediate. The attack can be directed either at the metal (this is equivalent to the inner-sphere pathway) or at the NO ligand (implying the outer-sphere pathway). Energetic arguments are clearly in favor of the dinitrosyl formation ($\Delta E = 18.2$ kcal/mol) than the direct coupling ($\Delta E = 12.2$ kcal/mol). However, since both reactants are paramagnetic, the spin density repartition turns out to play a crucial role in the reaction mechanism. The spin density contour calculated for the {Cu^INO}**M5** complex (Fig. 3) clearly shows the retention of the spin density on the NO ligand, as only 10% of the total spin density is delocalized over the metal-based orbitals. Therefore, the spin density repartition suggest that the attack of the paramagnetic NO molecule should be directed at the ligand. Indeed, comparison of the free valence indexes for Cu (FV = 0.015) and N centers (FV = 0.28) indicates that the nitrogen atom should be the preferred site for NO attack, favoring thereby a direct NO coupling. Furthermore, DFT calculations showed that it occurs with nearly zero activation energy. So that we may reasonably suppose that at low temperatures the dinitrosyls, if still present, are most probably the spectators, whereas the N_2O_2 species produced upon the direct coupling are the actual transients in the N–N bond formation process. It is worth mentioning here that N_2O_2 dimers were detected in gas phase [32] and in CuZSM-5 zeolite by IR spectroscopy as well [28].

A more detailed analysis of the IR data provided additional arguments for this conjecture. From our DFT studies it turned out that dinitrosyl species are rarely linear assuming usually either an *attracto* or *repulso* conformation [33], exemplified with the {$Cu^I(NO)_2$}**M7** cluster in Fig. 4a and b. A method of distinguishing between both conformers, which is based on

Table 1
NO stretching frequencies and magnetic parameters calculated for the {Cu^INO}Z complexes in various hosting sites of the ZSM-5 framework

Structure	ν (cm^{-1})	***g*** tensor			^{Cu}***A*** tensor (10^{-4} cm^{-1})				^{N}***A*** tensor (10^{-4} cm^{-1})			
		g_{xx}	g_{yy}	g_{zz}	a_{iso}	T_{xx}	T_{yy}	T_{zz}	a_{iso}	T_{xx}	T_{yy}	T_{zz}
{Cu^INO}**I2**	1768	2.011	2.016	1.916	168.7	−6.0	−24.7	30.7	11.3	18.1	−9.5	−8.6
{Cu^INO}**M5**	1777	2.011	2.019	1.904	158.7	−4.1	−19.0	23.1	11.7	19.1	−9.8	−9.3
{Cu^INO}**Z6**	1781	2.008	2.012	1.881	197.8	−5.2	−21.9	27.1	12.7	17.9	−9.3	−8.6
{Cu^INO}**M7**	1778	2.010	2.014	1.912	195.6	−8.7	−21.0	29.6	10.8	17.9	−9.2	−8.7
Experimental	1814	1.999	2.003	1.889	158.5	−9.0	−13.6	22.6	12.3	15.7	−8.3	−7.4

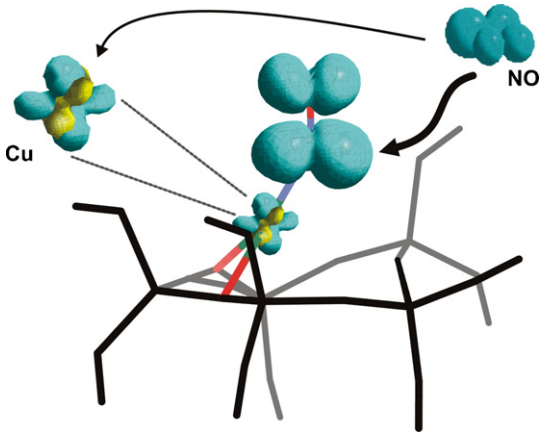

Fig. 3. BPW/DNP calculated spin density contours of the η^1-N\{^{2}Cu^{I}NO\}**M5** complex and NO molecule showing two possible routes of NO attachment: an inner-sphere attack at the metal center (narrow arrow) and outer-sphere attack at the NO ligand (bold arrow).

comparison of the intensity ratio of the antisymmetric and symmetric bands, is described below.

After binding of two NO molecules to copper(I), the resultant η^1-N\{Cu^I(NO)$_2$\}Z complex exhibited a pseudo-tetrahedral structure, typical also for analogous homogeneous complexes [34]. The first coordination sphere of the copper center is constituted by two framework oxygen ligands O$_z${Al, Si} located in the vicinity of aluminum atom along with two equivalent, angularly coordinated NO molecules (Fig. 4). In the case of the *repulso* conformation, the NO ligands are bent outwards, giving rise to the proximal-nitrogen and distal-oxygen atomic arrangement, whereas in the *attracto* form the NO ligands are bent inwards, bringing both oxygens close to ($d_{O–O}$ = 2.40 Å) and the nitrogen atoms away from each other. The *attracto* conformer was favored by 7.7 kcal/mol over the *repulso* one. This result is valid for all the copper hosting sites considered here (**I2**, **M5**, **Z6**, **M7**). The ground state of the {Cu^I(NO)$_2$}Z complex is a spin singlet, which implies an antiferromagnetic coupling of two paramagnetic NO ($^2\Pi_{1/2}$) ligands. The energy of the excited triplet state was calculated to be situated at 5.8 kcal/mol above the ground singlet state. This result is in line with EPR data, where with the increasing p_{NO} a steady decline in the intensity of the {Cu^{I}NO}ZSM-5 signal was observed, due to the formation of diamagnetic dinitrosyl species [35].

The basic geometrical characteristics of the *attracto* complexes are listed in Table 2. Regardless of the cluster type, the geometry of the geminal {Cu^I(NO)$_2$}Z moiety remains very similar. The N–O bond distance changes within a narrow range of 1.180–1.192 Å, the bending angle (α) of NO ligand is close to 125°, whereas the angle formed between two Cu–N bonds ($\theta_{N–Cu–N}$) equals to 92°. Slightly greater range of the $d_{Cu–N}$ values (1.911 ± 0.040 Å) does not alter geometry of the {Cu^I(NO)$_2$} unit much, though the shorter Cu–N bond lengths were found to correspond to the longer N–O distances.

One of the principal observables diagnostic for the interaction of NO with copper sites is the frequency of the valence vibrations of the resultant complexes. To link the observed IR spectra with the molecular models of the corresponding dinitrosyl adducts we analyzed the position of the bands, their width, and their intensity in more detail. Each of these parameters brings valuable piece of information in relation to the structure, speciation, and localization of the dinitrosyl species.

For the {Cu^I(NO)$_2$} moiety, the vibrational analysis raveled two collective normal modes well separated and not contaminated by other vibrations: a symmetric mode of the lower intensity and an antisymmetric one of the higher intensity. The results of the frequency calculations by DFT for the all investigated sites are collected in Table 3. A common feature of the calculated frequencies is a slight red shift of the bands with respect to the experimental values; however, the error does not exceed 4%. Similar accuracy has been achieved for the mononitrosyl complexes by other authors using embedded cluster approach [36] and more advanced QM-Pot

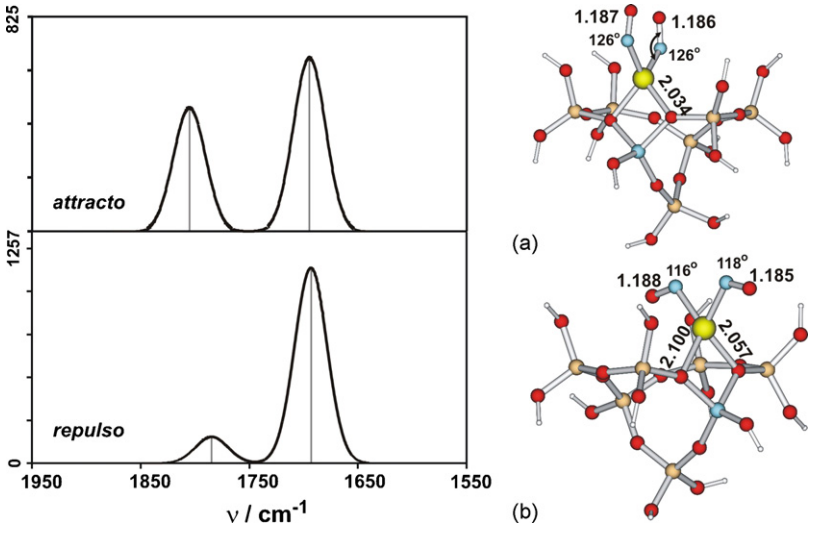

Fig. 4. Optimized BPW/DNP structures of the dinitrosyl adducts η^1-N\{^{1}Cu^I(NO)$_2$\}**M7** for (a) *attracto* and (b) *repulso* conformation, along with the corresponding calculated IR spectra in N–O bond stretching region. All bond lengths are given in angstroms, and angles, in degrees.

Table 2
Comparison of the adsorption energy and selected geometric parameters for the $\{Cu^{I}(NO)_2\}Z$ complexes in *attracto* conformation for various hosting sites of the ZSM-5 framework

Structure	ΔE_{ads} (kcal/mol)	d_{N-O} (Å)	d_{Cu-N} (Å)	α_{Cu-N-O} (°)	θ_{N-Cu-N} (°)
$\{Cu^{I}(NO)_2\}$**I2**	−18.2	1.186/1.188	1.910/1.911	125/125	92
$\{Cu^{I}(NO)_2\}$**M5**	−15.8	1.192/1.180	1.871/1.951	127/125	92
$\{Cu^{I}(NO)_2\}$**M7**	−16.7	1.183/1.186	1.936/1.883	124/126	92
$\{Cu^{I}(NO)_2\}$**Z6**	−19.0	1.187/1.186	1.911/1.912	126/126	92

Table 3
Calculated frequencies and intensities of the NO stretching vibrations for the $\{Cu^{I}(NO)_2\}Z$ complex for various hosting sites of the ZSM-5 framework

Structure	*Attracto*			*Repulso*		
	ν_{asym} (cm^{-1}) (intensity, km/mol)	ν_{sym} (cm^{-1}) (intensity, km/mol)	I_{sym}/I_{asym}	ν_{asym} (cm^{-1}) (intensity, km/mol)	ν_{sym} (cm^{-1}) (intensity, km/mol)	I_{sym}/I_{asym}
$\{Cu^{I}(NO)_2\}$**I2**	1673 (537.1)	1786 (383.7)	0.72	1673 (1143.1)	1766 (154.6)	0.14
$\{Cu^{I}(NO)_2\}$**M5**	1677 (556.2)	1801 (284.2)	0.51	1670 (1083.5)	1787 (192.9)	0.18
$\{Cu^{I}(NO)_2\}$**Z6**	1683 (568.3)	1799 (328.0)	0.58	1703 (1042.5)	1805 (192.5)	0.19
$\{Cu^{I}(NO)_2\}$**M7**	1678 (563.4)	1793 (330.5)	0.59	1689 (1165.7)	1785 (123.8)	0.11
Experimental	1730	1825	0.58			

methodology as well [37]. The average difference between the symmetric and antisymmetric vibration frequencies, equal to 110 cm^{-1}, is close to the experimental value of 95 cm^{-1}. Furthermore, the calculated values of ν_{sym} and ν_{asym} for various hosting sites within the zeolite structure show rather small variance ($\Delta\nu_{sym}$ = 15 cm^{-1} and $\Delta\nu_{asym}$ = 10 cm^{-1}). Thus, taking into account the experimental linewidth of 10 and 13 cm^{-1}, respectively, the band positions of the symmetric (ν_{sym}) and antisymmetric (ν_{asym}) components are virtually almost insensitive to the molecular environment of copper, and are thus not diagnostic either for the speciation or for the conformation of the nitrosyl complexes. This remains in agreement with the observed apparent homogeneity of the surface dinitrosyl complexes, reinforced by mere diagonal binding of the copper center to the zeolite framework upon coordination of NO.

Because of the lack of direct structure sensitivity of the stretching frequencies, for distinguishing between the *attracto* and *repulso* conformers of the $\{Cu^{I}(NO)_2\}$ZSM-5 complex we focused our attention on the IR peak intensities. From inspection of the data listed in Table 3 it is clear that the relative intensities of the symmetric and antisymmetric stretchings are markedly altered, whereas the band positions do not vary much with the conformation change for all the investigated sites.

Reliable prediction of IR intensities is much more demanding than locating the frequencies of the vibrational transitions. Within the so-called double-harmonic approximation [38], the intensity of an IR active transition can be associated with a mixed second derivative of the total energy with respect to the electric field and nuclear coordinates $I_i \sim |\partial E/(\partial \boldsymbol{E} \partial q_i)|^2$. Therefore, it is treated as a second-order property, which is typical for all current implementations of calculating the IR band strength. Commonly used GGA methods usually give the intensities accurate within ±10% only. In addition, the double-harmonic approximation introduces further uncertainty of about ±10% as well [39].

As we deal with two coupled vibrations, instead of the absolute intensities of the symmetric and antisymmetric bands, for further analysis we can utilize their ratio (I_{sym}/I_{asym}), in order to improve the accuracy. The DFT calculated values for both conformers and the value obtained after integration of the experimental spectra are summarized in Table 3. Two representative spectral profiles calculated for the *attracto* and *repulso* conformers of the $\{Cu^{I}(NO)_2\}$**M7** complex are presented in Fig. 4, along with the corresponding structures. As shown in Table 3, the intensity of the antisymmetric band is five times greater for the *repulso* form, whereas for the *attracto* conformer the intensities of both bands are more equilibrated. The calculated I_{sym}/I_{asym} ratio is very close to the experimental value for the *attracto* conformation only. Thus, the differences in the calculated I_{sym} and I_{asym} values for the $\{Cu^{I}(NO)_2\}Z$ complexes are much greater that the calculation uncertainties, and are therefore diagnostically significant. Comparison of the calculated (Fig. 4) and experimental IR spectra (Fig. 1) clearly shows that the copper dinitrosyls encaged in ZSM-5 exhibit the *attracto* conformation.

This type of geometry has already been suggested for dinitrosyl complexes of $3d^n$ transition-metal ions with good π-acceptor ligands. For such complexes the value of the θ_{N-Cu-N} angle has been found to be lower than 130°. On the contrary, the *repulso* adducts are characteristic of $4d^n$ and $5d^n$ complexes of transition-metal ions with poor π-acceptor ligands. The θ_{N-Cu-N} angle is usually greater than 130° in this case [33]. Commonly the value of the I_{asym}/I_{sym} ratio is used for estimating the angle between geminal ligands in the $\{M(XY)_2\}^n$ complexes, based on the approximate formula of Cotton and Wilkinson [40]:

$$\frac{I_{asym}}{I_{sym}} = \mathrm{tg}^2\left(\frac{\theta}{2}\right) \quad (1)$$

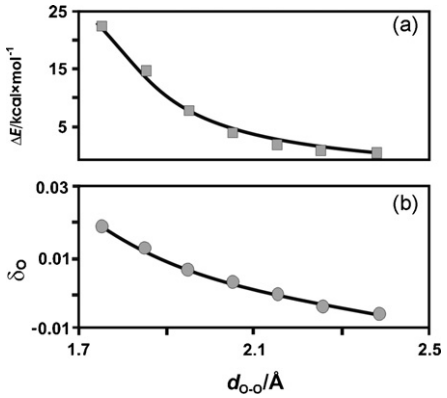

Fig. 5. The changes in (a) total energy and (b) partial charge on the terminal oxygen atoms of NO ligands calculated during the stepwise decrease of the O–O distance for the *attracto* dinitrosyl complex.

However, this equation is valid only in the case when the dipole moment of the adsorbed XY molecule and the direction of the bond defined by the arrangement of the M–X–Y atoms are collinear. This implies a η^1 linear mode of the XY bonding, such as that found in dicarbonyl complexes of copper [41,42]. In the case of copper dinitrosyls, exhibiting two angularly bound NO ligands, the θ angle obviously does not correspond to the $\theta_{N–Cu–N}$ angle, but to the angle that is defined by dipole moments of the coordinated NO molecules. Thus, the estimated value of the dinitrosyl angle for $\{Cu^I(NO)_2\}$ZSM-5 using Eq. (1) should not be identified with the $\theta_{N–Cu–N}$ angle, as made sometimes. Indeed, the values of the $\theta_{N–Cu–N}$ angle based on the Cotton formula ranges between 100° and 105° (Table 2), whereas the DFT calculated values of the actual $\theta_{N–Cu–N}$ angle, being virtually equal to 92° for the all optimized structures, are rather rigid (Table 2).

3.4. Mechanistic importance of the $\{Cu(NO)_2\}$ conformation

The spatial proximity of both oxygens in the *attracto* conformation may apparently suggest that the O–O bond formation could initiate the NO decomposition. However, the DFT results showed that once the oxygen–oxygen distance decreases, the positive charge develops on both terminal O-atoms, giving rise to steadily increasing energy due to the growing coulombic repulsion (Fig. 5a and b). We may conclude that the *attracto* conformation is an essentially inert form, and the NO decomposition cannot be initiated by the O–O bond formation step.

The alternative N–N bond making route entails a prior transformation of the *attracto* to *repulso* conformation. An approximate energy profile of this process (Fig. 6) was obtained by systematic variation of the appropriate reaction coordinate that was next kept frozen during the optimization of the rest of the cluster. As shown in Fig. 6, the transition state of the *attracto* to *repulso* transformation is located 13.4 kcal/mol above the *attracto* level, and assumes the geometry with two nearly linear NO ligands. Although the subsequent inner-sphere coupling of both NO ligands is energetically less demanding, requiring 6.0 kcal/mol only, the alternative outer-sphere coupling of the ligated NO with the gas-phase NO is barrierless. Thus, it turns out that kinetically the outer-sphere direct coupling should be favored over the more involved dinitrosyl pathway, which is preferred thermodynamically.

Having all the essential building blocks verified spectroscopically, we can commence modeling of the first mechanistic cycle of the *de*NO_x reaction, where NO reacting with $\{Cu^I\}Z$ center is transformed into N_2O. This process involves the following elementary steps:

$$\{Cu^I\}Z + NO_{(g)} \rightarrow \{Cu^INO\}Z \quad (2)$$

$$\{Cu^INO\}Z + NO_{(g)} \rightarrow \textit{cis}\text{-}\{Cu^IN_2O_2\}Z \rightarrow \textit{trans}\text{-}\{Cu^IN_2O_2\}Z \quad (3)$$

$$\{Cu^IN_2O_2\}Z \rightarrow \{(CuO)^I\}Z + N_2O_{(g)} \quad (4)$$

The total energy change for the overall reaction of $\{Cu^I\}$**M5** + 2NO → $\{CuO\}$**M5** + N_2O was equal to −47.3 kcal/mol. A more detailed energetic profile of this reaction is shown in Fig. 7, along with the proposed counterfeit

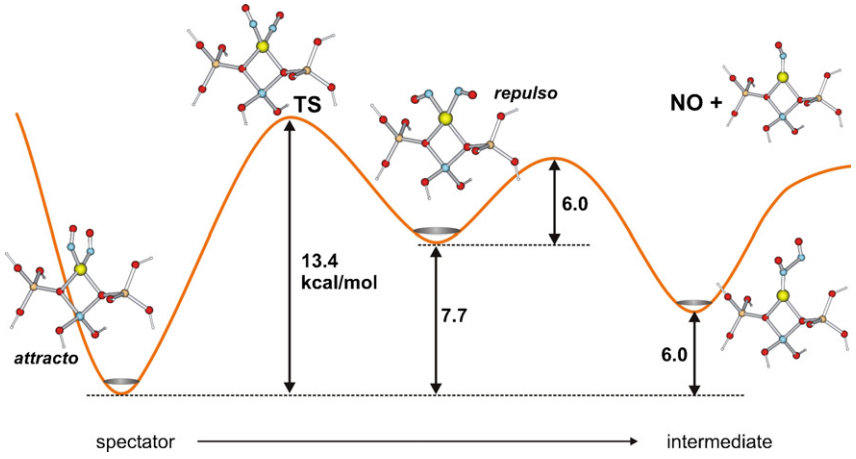

Fig. 6. Schematic potential energy profile for two types of the N–N bond formation mechanisms calculated for the **I2** hosting site.

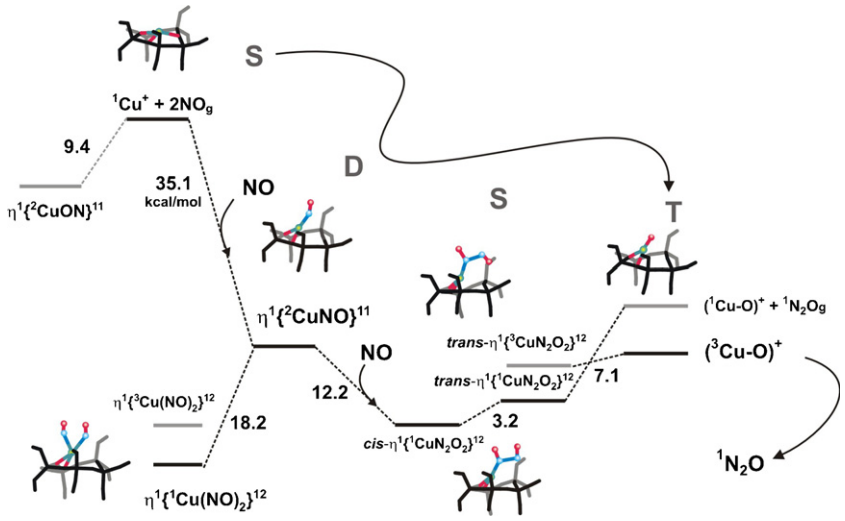

Fig. 7. Energy diagram of the reaction CuZSM-5 + 2NO → {CuO}ZSM-5 + N_2O including associated spin and conformation isomers calculated for the **M5** site. The values are given in kcal/mol. The letters S, D, and T indicate the singlet, doublet, and triplet states, respectively.

intermediate and spectator species (drawn in gray) for providing a suitable chemical reference context. The crucial steps of the N–N bond knitting include exoergic formation of the mononitrosyl complex (2), its transformation into $\{Cu^IN_2O_2\}Z$ transient via an outer-sphere NO coupling (3), and finally decomposition of copper bound N_2O_2 species into N_2O and the copper-oxo site (4). The latter process is kinetically constrained by the intersystem crossing, because the spin singlet $\{^1CuN_2O_2\}/Z$ intermediate is transformed into the $\{^3CuO\}Z$ center exhibiting a triplet ground state.

It is worth noting, that the N–N bond formation via dimeric N_2O_2 intermediate has already been postulated on the basis of spectroscopic results to take place on metallic surfaces [43,44] and in biological systems containing copper [45–47] and iron [48] as well. Also gas-phase NO decomposition supposedly occurs via dimer intermediates [49,50].

4. Conclusions

Interaction of NO with the Cu^IZSM-5 catalyst having mononuclear copper centers provides a useful functional model for experimental and theoretical investigations of the elementary processes involved in *de*NO_x reaction. Considerable insight into the nature of the active sites, the intermediates and the mechanism along which the N–N bond is formed (to produce a midway N_2O product) can be gained from joint use of spectroscopy and molecular modeling. The results obtained in this study support the view that the key transient $\{Cu^I(N_2O_2)\}$ZSM-5 is produced via an outer-sphere direct coupling of the copper-bound NO with the gas-phase NO. Basing on the in situ IR studies in static and flow regimes complemented by DFT calculations it is argued that copper mononitrosyl complexes play the role of the reaction intermediates, whereas the dinitrosyl complexes, formed only in the *attracto* conformation, are not involved in this process at the reaction conditions.

Acknowledgements

Financial support by the Committee for Scientific Research of Poland, KBN, Grant no. 3 T09A 147 26 is acknowledged. The calculations were carried out with the computer facilities of CYFRONET-AGH, the Academic Computing Center, under Grant no. KBN/SGI2800/UJ/018/2002. P. Pietrzyk thanks the Prime Minister of Poland for the Ph.D. Thesis Award.

References

[1] M. Iwamoto, S. Yokoo, K. Sakai, S. Kagawa, J. Chem. Soc. Faraday Trans. 77 (1981) 1629.
[2] M. Shelef, Chem. Rev. 95 (1995) 209.
[3] G. Turnes Palomino, P. Fisicaro, S. Bordiga, A. Zecchcina, E. Giamello, C. Lamberti, J. Phys. Chem. B 104 (2000) 4064.
[4] G. Busca, M.A. Larrubia, L. Arrighi, G. Ramis, Catal. Today 107–108 (2005) 139.
[5] M.V. Konduru, S.S.C. Chuang, J. Catal. 196 (2000) 271.
[6] P. DaCosta, B. Moden, G.D. Meitzner, D.K. Lee, E. Iglesia, Phys. Chem. Chem. Phys. 4 (2002) 4590.
[7] A.T. Bell, Catal. Today 38 (1997) 151.
[8] M.H. Groothaert, K. Pierloot, A. Delabiey, R.A. Schoonheydt, Phys. Chem. Chem. Phys. 5 (2003) 2135.
[9] P. Pietrzyk, Z. Sojka, J. Phys. Chem. A 109 (2005) 10571.
[10] Z. Sojka, M. Che, E. Giamello, J. Phys. Chem. B 101 (1996) 4831.
[11] M.H. Groothaert, J.A. van Bokhoven, A.A. Battiston, B.M. Weckhuysen, R.A. Schoonheydt, J. Am. Chem. Soc. 125 (2003) 7629.
[12] M.H. Groothaert, K. Lievens, H. Leeman, B.M. Weckhuysen, R.A. Schoonheydt, J. Catal. 220 (2003) 500.
[13] P.J. Smeets, M.H. Groothaert, R.A. Schoonheydt, Catal. Today 110 (2005) 303.
[14] C. Lamberti, S. Bordiga, G. Ricchiardi, M. Salvalaggio, G. Spoto, A. Zecchina, F. Geobaldo, G. Vlaic, M. Bellatreccia, J. Phys. Chem. B 101 (1997) 344.
[15] T. Spalek, P. Pietrzyk, Z. Sojka, J. Chem. Inf. Model. 45 (2005) 18.
[16] DMol, InsightII, Release 2000.1, Accelrys Inc., San Diego, CA, 2000.
[17] A.D. Becke, J. Chem. Phys. 88 (1988) 2547;
J.P. Perdew, Y. Wang, Phys. Rev. B 45 (1992) 13244.
[18] D. Nachtigallová, P. Nachtigall, M. Sierka, J. Sauer, Phys. Chem. Chem. Phys. 1 (1999) 2019.

[19] P. Pietrzyk, W. Piskorz, Z. Sojka, E. Broclawik, J. Phys. Chem. B 107 (2003) 6105.
[20] A.P. Scott, L. Radom, J. Phys. Chem. 100 (1996) 16502.
[21] M.J. Frisch, et al., Gaussian98, Revision A.6, Gaussian, Inc., Pittsburgh, PA, 1998.
[22] E. van Lenthe, P.E.S. Wormer, A. van der Avoird, J. Chem. Phys. 107 (1997) 2488.
[23] ADF2002.03, SCM, Theoretical Chemistry, Vrije Universiteit, Amsterdam, The Netherlands, http://www.scm.com.
[24] E. Giamello, D. Murphy, G. Magnacca, C. Morterra, Y. Shioya, T. Nomura, M. Anpo, J. Catal. 136 (1992) 510.
[25] J. Dědeček, Z. Sobalik, Z. Tvaružková, D. Kaucký, B. Wichterlová, J. Phys. Chem. 99 (1995) 16327.
[26] C. Prestipino, G. Berlier, F.X. Llabrés i Xamena, G. Spoto, S. Bordiga, A. Zecchina, G. Turnes Palomino, T. Yamamoto, C. Lamberti, Chem. Phys. Lett. 363 (2002) 389.
[27] K. Hadjiivanov, D. Klissurski, G. Ramis, G. Busca, Appl. Catal. B 7 (1996) 251.
[28] K. Hadjiivanov, Catal. Rev. -Sci. Eng. 42 (2000) 71.
[29] G. Spoto, S. Bordiga, D. Scarano, A. Zecchina, Catal. Lett. 13 (1992) 39.
[30] C. Henriques, M. Ribiero, C. Abreu, D. Murphy, F. Poignant, J. Saussey, J.C. Lavalley, Appl. Catal. B: Environ. 16 (1998) 79.
[31] M.V. Konduru, S.S.C. Chuang, J. Catal. 196 (2000) 271.
[32] A.R.W. McKellar, J.K.G. Watson, B.J. Howard, Mol. Phys. 86 (1995) 273.
[33] G.B. Richter-Addo, P. Legzdins, Metal Nitrosyls, Oxford University Press, New York, 1992.
[34] F.A. Cotton, G. Wilkinson, P.L. Gaus, Basic Inorganic Chemistry, John Wiley and Sons, Inc., 1987.
[35] V. Umamaheswari, M. Hartmann, A. Pöppl, J. Phys. Chem. B 109 (2005) 1537.
[36] E. Brocławik, J. Datka, B. Gil, P. Kozyra, Catal. Today 75 (2002) 353.
[37] M. Davidová, D. Nachtigallová, P. Nachtigall, J. Sauer, J. Phys. Chem. B 108 (2004) 13674.
[38] R.D. Amos, Molecular Property Derivatives, in: K.P. Lawley (Ed.), Ab Initio Methods in Quantum Chemistry—Part I, Wiley, Chichester, 1987.
[39] W. Koch, M.C. Holthausen, A Chemist's Guide to Density Functional Theory, Wiley/VCH, Weinheim, Germany, 2000.
[40] F.A. Cotton, G. Wilkinson, Advanced Inorganic Chemistry, Wiley, New York, 1980.
[41] A. Zecchina, S. Bordiga, G. Turnes Palomino, D. Scarano, C. Lamberti, M. Salvalaggio, J. Phys. Chem. B 103 (1999) 1519.
[42] K. Hadjiivanov, M. Kantcheva, D. Klissurski, J. Chem. Soc., Faraday Trans. 92 (1996) 4595.
[43] T.U. Bartke, R. Franchy, H. Ibach, Surf. Sci. 272 (1992) 299.
[44] A. Ludviksson, C. Huang, H.J. Jänsch, R.M. Martin, Surf. Sci. 284 (1993) 328.
[45] C.E. Ruggiero, S.M. Carrier, W.B. Tolman, Angew. Chem., Int. Ed. 33 (1994) 895.
[46] W.B. Tolman, Adv. Chem. Ser. 246 (1995) 195.
[47] P.C. Ford, I.M. Lorkovic, Chem. Rev. 102 (2002) 993, and references therein.
[48] R. Lin, P.J. Farmer, J. Am. Chem. Soc. 123 (2001) 1143.
[49] N. Tajima, M. Hashimoto, F. Toyama, A.M. El-Nahas, K. Hirao, Phys. Chem. Chem. Phys. 1 (1999) 3823.
[50] M.A. Vincent, I.H. Hillier, L. Salsi, Phys. Chem. Chem. Phys. 2 (2000) 707.